Noname manuscript No.
(will be inserted by the editor)

The hydra effect, bubbles, and chaos in a simple discrete population model with constant effort harvesting

Eduardo Liz · Alfonso Ruiz-Herrera

October 26, 2011

Abstract We analyze the effects of a strategy of constant effort harvesting in the global dynamics of a one-dimensional discrete population model that includes density-independent survivorship of adults and overcompensating density dependence. We discuss the phenomenon of bubbling (which indicates that harvesting can magnify fluctuations in population abundance) and the *hydra effect*, which means that the stock size gets larger as harvesting rate increases. Moreover, we show that the system displays chaotic behaviour under the combination of high per capita recruitment and small survivorship rates.

Keywords discrete population model · harvesting · bubbles · hydra effect · chaos.

Mathematics Subject Classification (2000) 92D25, 39A11, 39A33

1 Introduction

One dimensional maps have been very often used as models of population dynamics. Despite its apparent simplicity, it is well known that they can exhibit a rich dynamics (May 1976; Devaney 1989; Block and Coppel 1992). In many practical situations, besides the natural death rate of the population, there are other factors that increase the mortality; two clear examples are exploited populations of animals or plants (by harvesting or fishing), and the control of nuisance and invasive species. In these cases, the harvesting or culling rate is a new parameter that enters into the model and can be controlled to some

Eduardo Liz
Departamento de Matemática Aplicada II, E.T.S.I. Telecomunicación, Campus Marcosende, Universidad de Vigo, 36310 Vigo, Spain, E-mail: eliz@dma.uvigo.es

Alfonso Ruiz-Herrera
Departamento de Matemática Aplicada, Facultad de Ciencias, Universidad de Granada, 18071 Granada, Spain, E-mail: alfonsoruiz@ugr.es

extent. Thus, it is natural to study its influence in the dynamics taking it as a bifurcation parameter.

Some complex and sometimes counterintuitive effects of increasing mortality have been recently discussed; these include sudden collapses (Sinha and Parthasarathy 1996; Gyllenberg, Osipov and Söderbacka 1996; Schreiber 2001; Liz 2010b), paradoxical increases (Seno 2008; Abrams 2009; Liz 2010a; Sieber and Hilker (in press)), and transitions in the complexity of the dynamics (Dennis et al. 1997; Anderson et al. 2008; Zipkin et al. 2009).

While sudden collapses are typical of a strategy of constant quota harvesting, overcompensation and instabilities as a response to an increasing harvesting can occur in exploited populations with the more usual strategy of constant effort harvesting. Possibility of collapses due to saturating, constant effort harvesting in a Ricker model was first demonstrated by Schreiber (2003).

Ricker (1954) already suggested the possibility of an increasing in population abundance as a response to harvesting. We refer to Abrams (2009) for a recent survey about this phenomenon, which was also termed the *hydra effect.* In particular, Abrams illustrates these phenomena in discrete one dimensional models for nonoverlapping populations when harvesting occurs prior to reproduction (see also Seno 2008; Liz 2010a). We generalize these results to a model in which populations can overlap because a certain fraction of adults survive from time period to time period.

Regarding the influence of harvesting in the complexity of the system, it is commonly accepted that harvesting helps to stabilize the population, and this is indeed a characteristic of the usual one dimensional models (Goh 1977; May et al. 1978). However, some empirical studies have demonstrated the potential for increasing mortality to lead to instability in plant, insect and fish populations (see Zipkin et al. (2009), and references therein). Recent studies show that some discrete models with dimension higher than one can explain this phenomenon; for example, the three dimensional model for the flour beetle *Tribolium* analyzed by Dennis et al. (1997), and the two dimensional model employed by Zipkin et al. (2009). In both cases, an increasing adult mortality can destabilize the system. This is in accordance with the age-truncation hypothesis suggested by Anderson et al. (2008); using a one dimensional Ricker model, the authors explain a higher variability in population abundance as a result of fishing either by the influence of environmental fluctuations or by changes in the growth rates of the population. These two factors can amplify nonlinearity, and it is suggested that fishing may affect both.

In this paper, we show that instabilities as a result of increasing harvesting effort can be explained in a one-dimensional discrete model without considering external noise or changes in the demographic parameters, if survivorship of adults is allowed (thus considering a sort of age-structure); this model was suggested by Clark (1990, Section 7.5). Moreover, we identify the values of the intrinsic parameters of the model (growth rate, survivorship rate) for which this effect can be observed. This is linked to *bubble* structures (Bier and Bountis 1984; Vandermeer 1997; Ambika and Sujatha 2000), which appear when the usual route of period-doubling bifurcations to chaos is broken, and period-

halvings lead again the system to a stable equilibrium. Under the combination of high per capita recruitment and small survivorship rates, an increasing harvesting leads to an infinite creation and destruction of periodic orbits, in such a way that the bifurcation diagram shows paired period-doubling cascades, recently described by Sander and Yorke (2011). Using the notion of strictly turbulent functions (Block and Coppel 1992), we provide analytic results proving existence of chaos in the considered model for particular choices of the involved parameters.

The paper is organized as follows: in Section 2, we introduce the model and discuss some general properties; in Section 3, we analyze the hydra effect, the bubbling scenario, and complex behaviour; in Section 4 we give some concluding remarks. Some proofs and the analysis of chaotic dynamics are presented in two appendices.

2 The one-dimensional model

We consider a one-dimensional population model suggested by Clark (1990) (see also Thieme 2003; Liz 2010b), whose main characteristic is that assumes that the parent stock suffers only limited mortality from one period to the next, providing in this way a sort of age structure. We assume, as usual, harvest occurs prior to breeding (see Zipkin et al. (2009), and references therein). See Figure 1 (cf. p. 217 in Clark 1990).

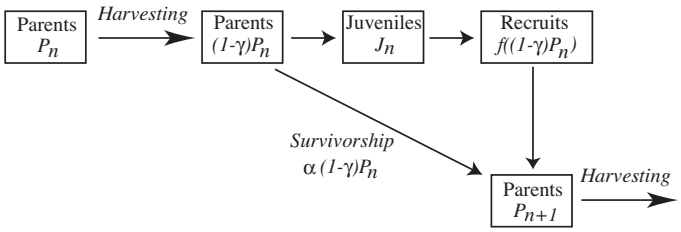

Fig. 1 Population model with parental survival and harvesting.

This model leads to a first-order difference equation

$$P_{n+1} = \alpha(1-\gamma)P_n + (1-\alpha)f((1-\gamma)P_n), \tag{1}$$

where $\alpha \in (0,1)$ is the *survivorship rate* of adults, $\gamma \in (0,1)$ is the *rate of harvesting,* f is the *stock-recruitment* function, and P_n represents the adult population after n generations, before harvesting. We are considering a strategy of constant effort harvesting; a discussion of a similar model with constant quota harvesting can be found in (Liz 2010b).

The parameter α can be interpreted as the fraction of energy invested into adult survivorship rather than reproduction. This interpretation assumes that density dependent survivorship only acts on juveniles; this is the case of the

Ricker model (Ricker 1954), which is based on the observation that certain species of fish as salmon habitually cannibalize their eggs and larvae.

The main advantage of this model is its simplicity, which allows us a better understanding of the dynamics, and the influence of the involved parameters, mainly, adult survivorship, rate of harvesting, and natural growth rate on population dynamics.

We consider that the density dependent stock-recruitment relationship is given by the Ricker map, which, after normalization, can be written as $f(x) = xe^{r(1-x)}$, where $r > 0$ is a growth rate parameter (see, e.g., Hastings 1997). Thus, our aim is to understand the effects of increasing mortality in equation

$$x_{n+1} = \alpha(1-\gamma)x_n + (1-\alpha)(1-\gamma)x_n e^{r(1-(1-\gamma)x_n)}, \tag{2}$$

depending on the values of the parameters $\alpha \in (0,1)$, and $r > 0$. The limit case $\alpha = 0$ corresponds to the usual Ricker model, where adults die after recruitment. A similar model to (1) was recently proposed by Yakubu et al. (2011) to assess the performance of a strategy of constant effort fishing; they show that equation (2) fits well to Atlantic cod data from the North East Fisheries Science Center.

If we define the map

$$F_\alpha(x) = \alpha x + (1-\alpha)xe^{r(1-x)}, \tag{3}$$

then equation (2) can be rewritten as

$$x_{n+1} = F_\alpha((1-\gamma)x_n). \tag{4}$$

In some cases when γ is the relevant parameter, we will denote $h_\gamma(x) = F_\alpha((1-\gamma)x)$. Some properties of the map F_α and the dynamics generated by it were recently studied; in the next proposition, we list some of them for future reference. For their proofs, we refer to Appendix B of (Liz 2010b) and Appendix A of (Liz and Franco 2010).

Proposition 1 *Let $\alpha \in [0,1)$. The following properties hold for the map F_α defined in (3):*

(a) *F_α has two fixed points: $x = 0$ and $x = 1$. Moreover, $F_\alpha(x) > x$ for all $x \in (0,1)$, and $F_\alpha(x) < x$ for all $x > 1$.*

(b) *F_α is nondecreasing or bimodal, with two critical points $0 < c_1 < c_2$ such that F_α is decreasing on (c_1, c_2). Moreover, $(SF_\alpha)(x) < 0$ for all $x \in (c_1, c_2)$, where*

$$(SF_\alpha)(x) = \frac{F'''_\alpha(x)}{F'_\alpha(x)} - \frac{3}{2}\left(\frac{F''_\alpha(x)}{F'_\alpha(x)}\right)^2$$

is the Schwarzian derivative of F_α.

In the next result we provide some useful information concerning the equilibria of equation (4) and their stability. As usual, we say that a positive equilibrium K of (2) is globally stable if it is asymptotically stable and all solutions of equation (2) starting at a positive initial condition converge to K.

Theorem 1 *For each $r > 0$ and $\alpha \in [0, 1)$, let us define*

$$\gamma^* = \gamma^*(r, \alpha) := 1 - \frac{1}{F'_\alpha(0)} = 1 - \frac{1}{(1-\alpha)e^r + \alpha}\,. \tag{5}$$

The following statements hold:

(i) If $\gamma \geq \gamma^*$ then all solutions of equation (2) converge to zero.
(ii) If $\gamma < \gamma^*$ then zero is unstable and equation (2) has a unique positive equilibrium

$$K_\gamma = \frac{1}{1-\gamma}\left[1 - \frac{1}{r}\ln\left(\frac{1-(1-\gamma)\alpha}{(1-\alpha)(1-\gamma)}\right)\right]. \tag{6}$$

(iii) If $\gamma < \gamma^*$ and $(1-\gamma)F'_\alpha((1-\gamma)K_\gamma) \geq -1$ then the positive equilibrium K_γ is globally stable.
(iv) If $\gamma < \gamma^*$ and $(1-\gamma)F'_\alpha((1-\gamma)K_\gamma) < -1$ then the positive equilibrium K_γ is unstable.

The proof of Theorem 1 is given in Appendix A. Notice that properties (iii) and (iv) mean that K_γ is globally stable if and only if it is locally asymptotically stable.

We can derive a couple of immediate consequences about model (1) from the above stated results; on the one hand, overharvesting leads the population to extinction; on the other hand, a big enough harvesting effort stabilizes the system about a globally attracting positive equilibrium.

If we denote

$$r_0(\gamma) = \ln\left(\frac{1-(1-\gamma)\alpha}{(1-\alpha)(1-\gamma)}\right), \tag{7}$$

then the condition for extinction $\gamma \geq \gamma^*$ is equivalent to $r \leq r_0(\gamma)$. It follows from statement (iii) in Theorem 1 that K_γ is globally stable if

$$r_0(\gamma) < r \leq \frac{2}{1-\alpha(1-\gamma)} + r_0(\gamma)\,.$$

Since $\gamma \geq 0$ implies that $r_0(\gamma) \geq 0$, K_γ is globally stable for $r \leq 2$ (whenever it exists) regardless the values of $\alpha \in (0, 1)$ and $\gamma \in (0, 1)$. Thus, harvesting cannot destabilize the population at low growth rates.

3 The hydra effect, bubbles, and chaos

In this section we analyze the potential of equation (2) to produce the phenomena mentioned in the Introduction: the hydra effect, bubbles, and chaos.

3.1 The hydra effect

The phenomenon of an increasing population size in response to an increase in the per-capita mortality rate was named the *hydra effect* by Abrams and Matsuda (see Abrams (2009), and references therein) in allusion to the mythological beast that grew two heads to replace each one that was removed. Abrams (2009) has reviewed the mechanisms underlying the hydra effect; in particular, this effect was observed in overcompensatory discrete population models when mortality precedes density dependence, both when the positive equilibrium is asymptotically stable, and in systems that cycle. In the former case, the hydra effect means that the positive equilibrium gets larger as the mortality parameter increases. In order to provide a precise definition of the hydra effect for non-equilibrium dynamics, we formulate the discrete-time analog of some definitions recently introduced by Sieber and Hilker (in press) for continuous population models. To do this, we denote by $\{x_n(\gamma)\}_{n\geq 0}$ the solution of (2) for a given parameter $\gamma \in (0,1)$ and an initial condition $x_0 \geq 0$.

Definition 1 The mean value map is defined as the function $\phi : M \times (0,1) \to [0,\infty)$ given by

$$\phi(x_0,\gamma) = \lim_{n\to\infty} \frac{1}{n} \sum_{i=0}^{n-1} x_i(\gamma),$$

where $M \subset [0,\infty)$ is the subset of initial conditions for which the previous limit exists.

The mean value map assigns to an initial condition x_0 and a harvesting rate γ the asymptotic mean value of the solution $\{x_n(\gamma)\}_{n\geq 0}$. It is clear that if K_γ is an equilibrium of (2) then $\phi(K_\gamma,\gamma) = K_\gamma$, and, if $\{x_n\}$ is a periodic solution with prime period m then $\phi(K_\gamma,\gamma) = (1/m)\sum_{i=0}^{m-1} x_i$.

Regarding the hydra effect, we consider a concept slightly different from Definition 3 in (Sieber and Hilker, in press).

Definition 2 (Hydra effect)

1. The population governed by (2) experiences a hydra effect over an interval $I \subset [0,1]$ if there is an initial condition x_0 such that the map $\gamma \mapsto \phi(x_0,\gamma)$ is increasing on I.
2. We say that a hydra effect occurs in a subset D of $(0,\infty)$ over an interval I if the previous statement holds for all $x_0 \in D$.

An interesting example is the case $\alpha = 0$ of (2), that is, the Ricker model with constant effort harvesting

$$x_{n+1} = (1-\gamma)x_n e^{r(1-(1-\gamma)x_n)}. \tag{8}$$

Seno (2008) proved that the positive equilibrium K_γ of (8) is globally stable and gets larger as γ increases if and only if $r > 1$ and $\gamma \in (1-e^{2-r}, 1-e^{1-r}) \cap (0,1)$. However, K_γ actually increases with γ for all $\gamma \in (0, 1-e^{1-r})$, although it is unstable for $\gamma \in (0, 1-e^{2-r})$ if $r > 2$ (see Liz 2010a).

Since it is known that the positive equilibrium of (8) equals the average population size even in the case of chaotic dynamics (see, e.g., Gyllenberg, Hanski, and Lindström 1996), it follows that, in the terms of Definition 1, for equation (8) we have $M = [0, \infty)$ and

$$\phi(x_0, \gamma) = \begin{cases} K_\gamma & \text{if } x_0 > 0 \text{ and } 0 < \gamma < \gamma^* = 1 - e^{-r}, \\ 0 & \text{if } x_0 = 0, \text{ or } x_0 > 0 \text{ and } \gamma \in [\gamma^*, 1). \end{cases}$$

Thus, for equation (8), there is a hydra effect in $(0, \infty)$ over the interval $(0, 1 - e^{1-r})$ (see the case $\alpha = 0, r = 4$ in Figure 3).

Equation (2) with $\alpha > 0$ does not share the same property about the mean population value in the Ricker model, and it can happen that, as harvesting is increased, the positive equilibrium gets larger while the mean population size decreases (see Figure 3); however, our numerical simulations suggest that the relationship $\phi(x_0, \gamma) \geq K_\gamma$ holds for all $x_0 > 0$ and $\gamma < \gamma^* = 1 - 1/((1 - \alpha)e^r + \alpha)$ (see again Figure 3, and also Figures 4–8).

When the positive equilibrium K_γ of (2) is asymptotically stable (and hence globally stable, by Theorem 1), a rigorous analysis of the hydra effect is easy to obtain. When K_γ is unstable, we discuss the occurrence of a hydra effect based on numerical simulations.

In the next result, we consider the case when K_γ is globally stable.

Proposition 2 *A hydra effect in equation (2) occurs in* $(0, \infty)$ *over an interval* (γ_1, γ_2) *defined implicitly by the inequalities*

$$\frac{1}{1 - \alpha(1 - \gamma)} + r_0(\gamma) < r \leq \frac{2}{1 - \alpha(1 - \gamma)} + r_0(\gamma)\,, \tag{9}$$

where $r_0(\gamma)$ *is defined in (7).*

Moreover, if

$$r \leq \frac{1}{1 - \alpha(1 - \gamma)} + r_0(\gamma) \tag{10}$$

then equation (2) does not experience a hydra effect at any point $x_0 \geq 0$.

Proof Theorem 1 ensures that the positive equilibrium K_γ is globally stable if the second inequality in (9) holds. Thus there is a hydra effect if and only if K_γ increases with γ. Differentiating the right-hand side of (6) with respect to γ, it follows that $\partial K_\gamma / \partial \gamma > 0$ if and only if the first nequality in (9) holds.

On the other hand, if (10) is true then it follows from Theorem 1 that either the positive equilibrium is globally stable or all solutions converge to zero. Since $\partial K_\gamma / \partial \gamma \leq 0$, a hydra effect cannot occur.

Proposition 2 allows us to represent in the plane of parameters (γ, α) the values for which there is a hydra effect in equation (2) for each fixed r when the positive equilibrium is globally stable. In Figure 2, we do it for $r = 4$. There is a hydra effect when γ ranges over intervals joining (α, γ_1) with (α, γ_2) which lie between the lower solid line and the dashed line. Hydra effect does not occur over horizontal segments included in the region above the dashed line.

A similar diagram can be produced for any $r > 2$. For $1 < r \leq 2$, the lower solid line disappears (because the positive equilibrium cannot be unstable), and then the region below the dashed line determines the intervals for which there is a hydra effect.

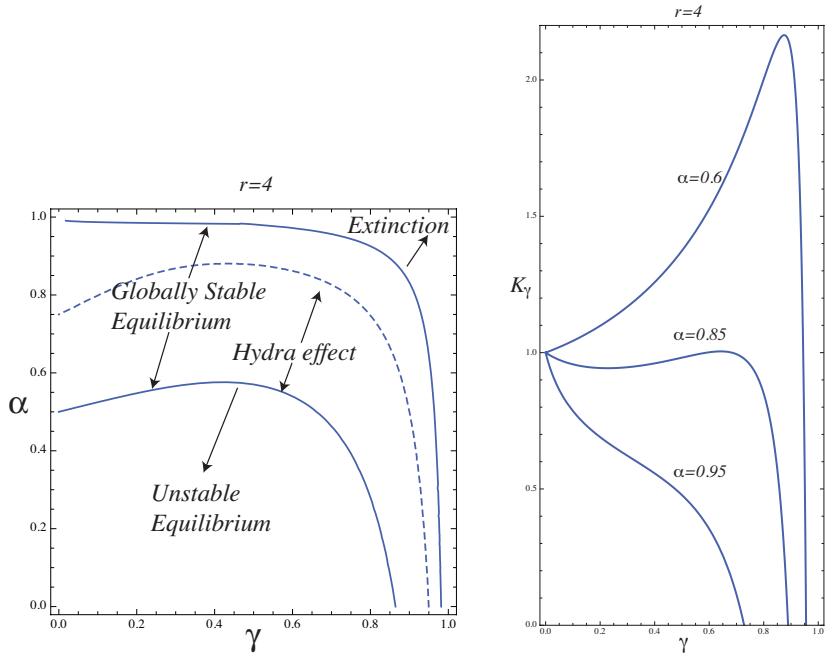

Fig. 2 Left: Regions of stability and the hydra effect in the plane of parameters (γ, α) for equation (2) with $r = 4$. Right: Variation of the positive equilibrium as γ is increased in equation (2) for $r = 4$, and different values of α.

In Figure 2 (right) we show how the equilibrium varies with γ for $r = 4$ and $\alpha = 0.6, 0.85, 0.95$. In the three cases, the positive equilibrium is always globally stable (when it exists) but the magnitude of the effect in the equilibrium as γ increases is quite different.

Figure 2 suggests some words of caution if one uses model (2) to justify that increasing harvesting is a good strategy to increment the population stock: the transition between the value of γ at which the population size at the equilibrium is maximum and the critical γ after which population is doomed to extinction is very fast. A similar comment applies to Figure 3.

As mentioned before, a hydra effect can also occur when K_γ is unstable (and hence, in general, $\phi(x_0, \gamma) \neq K_\gamma$). Our simulations show that occurrence of hydra effect in the unstable region of Figure 2 is irregular. In Figure 3 we represent the mean population abundance for $r = 4$ and four different choices of α, choosing the initial condition $x_0 = 0.5$. While for $\alpha = 0$ the equality $\phi(x_0, \gamma) = K_\gamma$ holds, and then there is a hydra effect over the interval

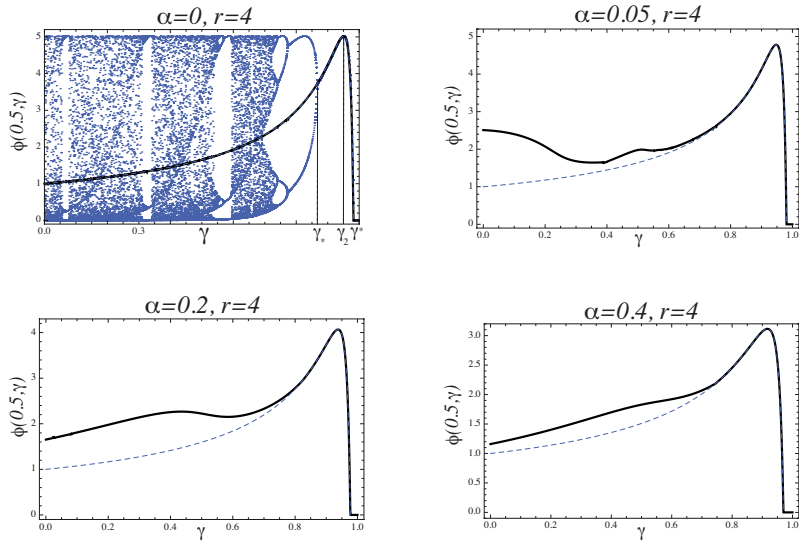

Fig. 3 Variation of the mean population abundance as γ is increased in equation (2) for $r = 4$, and different values of α. The solid lines represent the mean value $\phi(0.5, \gamma)$; the dashed lines correspond to the unstable equilibrium. In the case $\alpha = 0$, the mean value coincides with the equilibrium even when the equilibrium is unstable. We have included the bifurcation diagram to make clear the region of instability. The key values represented in the γ-axis are $\gamma_* = 1 - e^{-2}$, where the equilibrium becomes stable after a period-halving bifurcation, $\gamma_2 = 1 - e^{-3}$, until which there is a hydra effect, and $\gamma^* = 1 - e^{-4}$, after which the total population is driven to extinction.

$[0, 1 - e^{-3})$, for small positive values of α the mean abundance can decrease for small values of γ (see the case $\alpha = 0.05$ in the figure). As the value of α is increased, we observe a hydra effect except for an interval of intermediate values of γ (see the case $\alpha = 0.2$). Finally, for values of α close to the region of stability of the equilibrium, equation (2) seems to display a hydra effect over a large subinterval of $[0, 1]$, as in the case $\alpha = 0$ (see the case $\alpha = 0.4$).

Different choices of the initial condition x_0 provide exactly the same profiles for the mean population abundance. Thus, we guess that when hydra effect occurs in equation (2), it holds for almost all positive initial conditions. For $\alpha = 0$, this is a consequence of the fact that $F_0(x) = xe^{r(1-x)}$ is a unimodal map with negative Schwarzian derivative; see, e.g., the nice survey of Thunberg (2001). Although for all $\alpha \in (0, 1)$ a locally stable equilibrium of (2) is globally stable, similar results for arbitrary periodic orbits of bimodal maps do not seem to be available in the literature.

3.2 Bubbles and chaos

The period-doubling route to chaos is a very well-known feature in discrete dynamical systems, especially in the quadratic family $f(x) = rx(1 - x)$, with r ranging between 2 and 4 (see, e.g., Devaney 1989). Bier and Bountis (1984)

showed that in simple nonlinear discrete dynamical systems involving the variation of two or more parameters, the period-doubling process can be broken, giving rise to period-halving bifurcations, which in turn stabilize the system around an equilibrium point or a periodic solution. Thus, the bifurcation diagram forms closed loop-like structures similar to bubbles, and the effect is usually referred to as bubbling (see, e.g., Figure 4). The possibility for bubbling in families of maps depending smoothly on a parameter was already noted by Devaney (1989); cf. Remark in p. 154 and Figure 19.2 in p. 155. For more discussions and related references, see Ambika and Sujatha (2000).

The bubbling effect was found in several papers in an ecological context, besides those already mentioned in the Introduction. For example, Stone (1993) and Stone and Hart (1999) observed this effect in the usual one-dimensional models of population dynamics when a constant migration is considered; Vandermeer (1997) showed that quartic maps resulting from the composition of two logistic maps can exhibit bubbling; a similar effect in two-dimensional discrete models was found by Newman et al. (2002) for a population with a refuge, and by Schreiber (2007) for a host-parasitoid system.

Although the terms *bubble* and *bubbling* have been widely employed, we did not find a formal definition in the literature. We give a definition for one-dimensional maps depending on a parameter. Consider a family $f_\lambda : I \to I$ of $\mathcal{C}^1$-maps defined on a real interval I and depending smoothly on a parameter $\lambda \in \Lambda$, where Λ is a real interval too. We assume that, for each value of λ, there is a compact attracting invariant interval for f_λ, in such a way that the ω-limit set $\omega_\lambda(x_0)$ of any initial condition $x_0 \in I$ is invariant, nonempty and compact. Assume also that there is an interval $J \subset \Lambda$ and $\lambda_1, \lambda_2 \in J$ such that f_λ has a continuous branch of equilibria K_λ satisfying $|f'_\lambda(K_\lambda)| > 1$ for all $\lambda \in (\lambda_1, \lambda_2)$, and $|f'_\lambda(K_\lambda)| < 1$ for all $\lambda \in J \setminus (\lambda_1, \lambda_2)$.

Definition 3 In the above conditions, we say that the family $\{f_\lambda\}_{\lambda \in J}$ exhibits bubbling if, for some $x_0 \in I$, $\omega_\lambda(x_0) = K_\lambda$ for all $\lambda \in J \setminus (\lambda_1, \lambda_2)$, and $M(\lambda, x_0) := \max \omega_\lambda(x_0) > \min \omega_\lambda(x_0) := m(\lambda, x_0)$ for all $\lambda \in (\lambda_1, \lambda_2)$.

In this case, the set

$$B = \left(\bigcup_{\lambda_1 < \lambda < \lambda_2} (\lambda, m(\lambda, x_0)) \right) \bigcup \left(\bigcup_{\lambda_1 < \lambda < \lambda_2} (\lambda, M(\lambda, x_0)) \right)$$

is called a bubble.

The trace of a bubble may be discontinuous, that is, the maps $\lambda \mapsto m(\lambda, x_0)$ and $\lambda \mapsto M(\lambda, x_0)$ may exhibit jump discontinuities e.g. if there are saddle-node bifurcations.

The dynamics of f_λ for values of $\lambda \in (\lambda_1, \lambda_2)$ inside a bubble can be very simple or even chaotic; see, e.g., Figures 4 and 6. The simplest bubble, illustrated by Figure 4, is called a *primary bubble*. It is characterized by the fact that $\omega_\lambda(x_0)$ is a periodic orbit of prime period two $\{x_1(\lambda), x_2(\lambda)\}$, with $x_1(\lambda) < K_\lambda < x_2(\lambda)$, for every value of $\lambda \in (\lambda_1, \lambda_2)$. If the branches of 2-periodic orbits experience other period-doubling followed by period-halving

bifurcations on the interval (λ_1, λ_2), then secondary bubbles appear (Bier and Bountis 1984); see Figure 6.

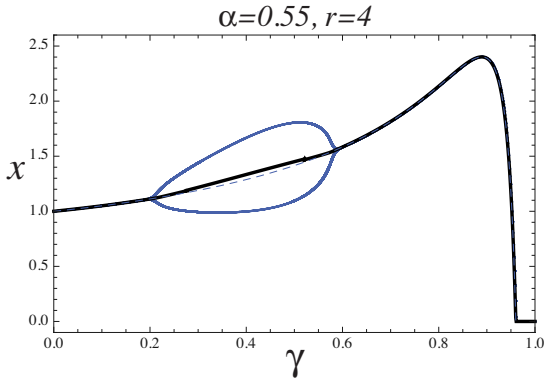

Fig. 4 Primary bubble in equation (2) with $r = 4$ and $\alpha = 0.55$ as γ is increased. The dashed line corresponds to the unstable equilibrium, and the thick line is the mean population abundance, which coincides with the equilibrium when it is asymptotically stable.

When a bubble exists, the equilibrium typically losses and regains its stability in two period-doubling bifurcations, where $f'_\lambda(K_\lambda) = -1$. This fact, together with property (b) of Proposition 1, ensures the existence of a stable 2-periodic orbit for values of $\lambda \in (\lambda_1, \lambda_2)$ close to λ_1 and λ_2; see, e.g., Theorem 12.7 and Remark 2 below Corollary 12.8 in (Devaney 1989). Thus, for fixed values of r and α, bubbles appear in equation (2) as γ is increased if and only if there are two values $0 < \gamma_1 < \gamma_2 < 1$ such that $h'_{\gamma_i}(K_{\gamma_i}) = -1$, for $i = 1, 2$, where $h_\gamma(x) = F_\alpha((1-\gamma)x)$.

Since, by Theorem 1, the positive equilibrium of (2) is globally stable for sufficiently large values of γ, bubbling is an appropriate mathematical concept to show that increasing mortality can lead to instability in (2). Zipkin et al. (2009) found bubble-type structures in the numerical study of a discrete population model with two stages (juveniles and adults), when adult mortality is increased. We show the same phenomenon for the simpler one-dimensional model (1).

The next result provides the values of the parameters r and α for which (2) exhibits bubbling.

Theorem 2 *Equation (2) exhibits bubbling for fixed values of r and α as γ is increased if and only if $r > 3$ and*

$$\alpha_1(r) := 1 - \frac{2}{r} < \alpha < \frac{e^{r-3}}{2 + e^{r-3}} := \alpha_2(r)\,. \tag{11}$$

We give the proof of Theorem 2 in Appendix A. Figure 5 (left) shows the range of values of α for which equation (2) exhibits bubbling as γ is increased, for r between 3 and 10. For example, for $r = 4$, there is bubbling

when $\alpha \in (0.5, 0.576)$. For $\alpha > 0.576$ the positive equilibrium is globally stable (when it exists) regardless the value of α, while for $\alpha < 0.5$ the equilibrium may be unstable but bubbling is not possible. In the right-hand side of Figure 5, we show this range in the plane (γ, α). A primary bubble for $\alpha = 0.55$ is numerically observed in Figure 4.

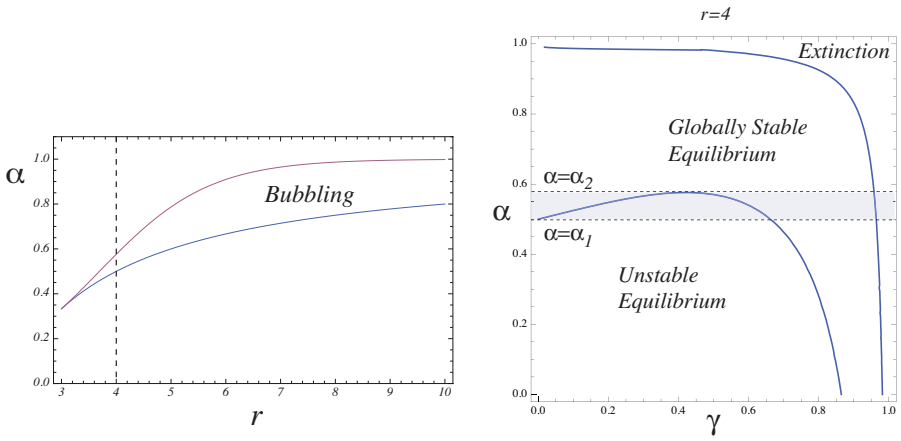

Fig. 5 Left: Range of values (r, α) for which bubbling occurs as γ is increased in equation (2), for $r \in (3, 10)$. The dashed line corresponds to the value $r = 4$ considered in the diagram on the right. Right: Regions of stability in the plane of parameters (γ, α) for equation (2) with $r = 4$. The shaded band between the lines $\alpha = \alpha_1(4)$ and $\alpha = \alpha_2(4)$ represents the values of α for which bubbles exist as γ is increased.

In Figure 6 (left), we represent the bifurcation diagram for equation (2) with $r = 6$ and $\alpha = 0.73$, showing secondary bubbles. Moreover, our numerical simulations suggest that harvesting can magnify fluctuations from a globally stable equilibrium to chaotic oscillations; see Figure 6 (right); we call the structures in the bifurcation diagram *chaotic bubbles*. This means that the period-halving bifurcations start after the family of maps g_γ has reached a chaotic regime. Chaotic bubbles are sometimes referred to as Feigenbaum remerging trees (Bier and Bountis 1984; Thamilmaran and Lakshmanan 2002). More recently, these structures were called paired period-doubling cascades (Sander and Yorke 2011).

The result stated in Theorem 2 is in agreement with numerical results found by Zipkin et al. (2009) for a two dimensional stage-structured model, namely, that instability as a result of harvest occurs in the case of adult-only harvest when both maximum per capita recruitment and adult survivorship are high. Zipkin et al. also claimed that no harvest strategy could cause instability in a population when adult survivorship was low. Although it is true that bubbling is not possible for $\alpha < 1/3$ in (2), this fact does not mean that harvesting does not magnify fluctuations of population abundance. For small survivorship rates, we observe numerically bubbles for the second iteration $h_\gamma^2 = h_\gamma \circ h_\gamma$ of the map $h_\gamma(x) = F_\alpha((1-\gamma)x)$, thus destabilizing a stable 2-

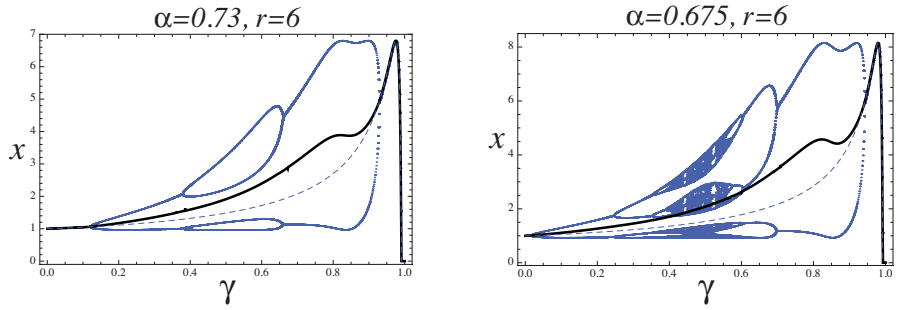

Fig. 6 Bubbling scenario in equation (2) with $r = 6$ as γ is increased. Left: secondary bubbles for $\alpha = 0.73$; right: chaotic bubbles for $\alpha = 0.675$. In both cases, the dashed line corresponds to the unstable equilibrium, and the thick line is the mean population abundance.

periodic orbit of (2). This fact also indicates that variability in the population size increases as γ is increased. See Figure 7.

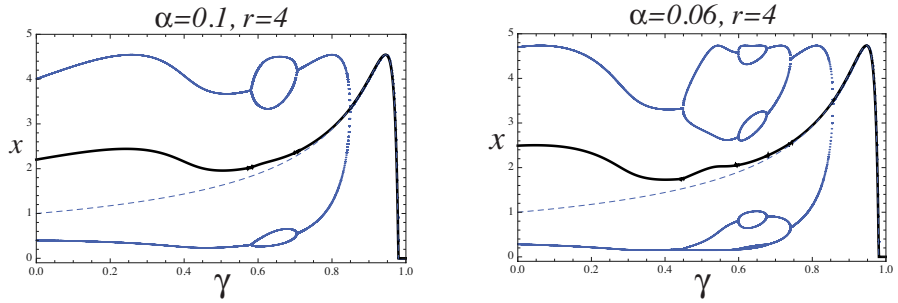

Fig. 7 Bubbles for the second iteration of $h_\gamma(x) = F_\alpha((1-\gamma)x)$ with $r = 4$ and small survivorship rates. In both cases, the dashed line corresponds to the unstable equilibrium, and the thick line is the mean population abundance.

For even smaller adult survivorship rates, our numerical simulations show that there are chaotic bubbles for h_γ^2. In Figure 8, for equation (2) with $r = 4$ and $\alpha = 0.02$, we can observe two period-five paired cascades between $\gamma = \gamma_a \approx 0.486$ and $\gamma = \gamma_b \approx 0.605$. At γ_a and γ_b, two period-five cycles are created and destroyed, respectively, in two period-five saddle-node bifurcations. The stable cycle undergoes infinitely many period doublings followed by period halvings, giving place to paired cascades. We show a detail on the right, including the branch of unstable periodic points. We refer to Sander and Yorke (2011) for precise definitions and results on paired cascades. Figure 8 illustrates that increasing harvesting at low survivorship rates can enhance variability in the population size from a simple period-two regime to a complex dynamics.

The numerical bifurcation diagrams shown in Figure 8 suggest that the dynamics of equation (2) with $r = 4$ and $\alpha = 0.02$ is chaotic for some values of

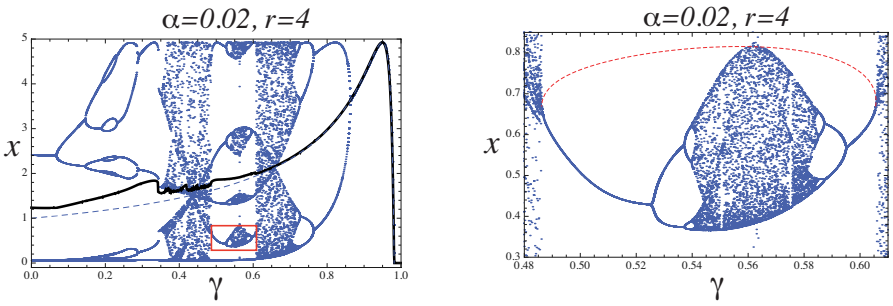

Fig. 8 Chaotic bubbles for h^2_γ with $r = 4$ and survivorship rate $\alpha = 0.02$. On the left, the parameter γ ranges from 0 to 1; we can observe two period-five paired cascades (as usual, the dashed line corresponds to the unstable equilibrium, and the thick line is the mean population abundance). On the right, we show a zoom of the small box on the left; the curve of unstable period five points is also displayed (red dashed line) to emphasize the critical values of γ where two period-five saddle-node bifurcations occur.

the harvesting parameter γ. In Appendix B, we rigorously prove that model (2) with $r = 4$, $\alpha = 0.02$, and $\gamma = 0.55$ is chaotic, and, due to the robustness of our approach, the same is true for a set of nearby values of the parameters.

The bifurcation diagrams displayed in Figures 4–8 indicate that bubbling and hydra effects often co-occur. Actually, a decrease in the mean population size as γ increases seems to happen almost only for intervals of the parameter γ inside a stable stationary or periodic regime, but not when a bubble is created.

Finally we note that, while the hydra effect in discrete population models usually requires that mortality precedes density dependence (Abrams 2009), bubbling occurs in the same parameter range if reproduction precedes harvesting. Indeed, if we consider equation

$$x_{n+1} = (1-\gamma)F_\alpha(x_n), \tag{12}$$

where F_α is defined in (3), then, for each value of γ, equations (2) and (12) are topologically conjugated by the homeomorphism $\psi(x) = (1-\gamma)x$. In particular, K_γ is a positive equilibrium of (2) if and only if $P_\gamma = (1-\gamma)K_\gamma$ is a positive equilibrium of (12); moreover, P_γ and K_γ have the same stability properties. In Figure 9, we represent two bubbles for $r = 4$ and $\alpha = 0.55$; the upper one corresponds to equation (2), and the lower one to equation (12). It is easy to check that there is no hydra effect in equation (12) when the equilibrium is stable, because $\partial P_\gamma/\partial\gamma < 0$ for all $\gamma \in (0, 1)$. Numerical simulations show that a hydra effect occurs very rarely in equation (12) also when the positive equilibrium is unstable.

4 Discussion

It is clear that exploited populations exhibit changes in their abundance in response to harvesting. Moreover, both empirical and theoretical observations

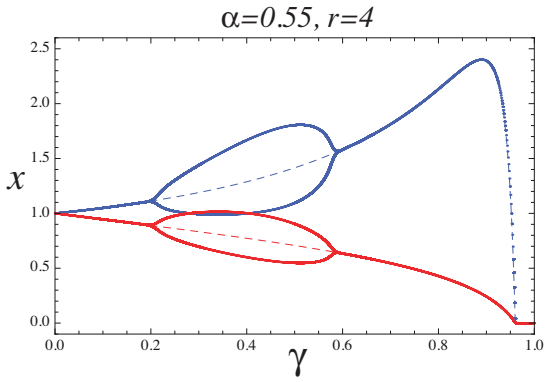

Fig. 9 Primary bubbles in equations (2) and (12) with $r = 4$ and $\alpha = 0.55$ as γ is increased. The dashed lines inside the bubbles correspond to the unstable equilibria. The upper bubble (blue online) corresponds to model (2), when harvesting occurs prior to reproduction; the lower one (red online) corresponds to equation (12), when harvesting occurs after reproduction.

have demonstrated that these changes are often unexpected and counterintuitive.

It is remarkable that simple one-dimensional discrete models serve as a paradigm of most of these phenomena; for a strategy of constant quota harvesting in a discrete model for a population without adult survivorship (such as the Ricker model), Schreiber (2001) provided a complete classification of the dynamics, which includes sudden collapses and essential extinction windows. Recently, Liz (2010b) showed that the effects of constant harvesting in the dynamics becomes even more complex when it is assumed that adult population undergoes only limited mortality from one period to the next.

In this paper, we have investigated the effects of an strategy of constant effort harvesting, which is usually employed in fisheries (Clark 1990). For it, we have considered a discrete model with density-independent survivorship of adults and overcompensating density dependence. Our main findings are the following:

On the one hand, assuming that harvesting occurs prior to breeding, the population abundance can get larger in response to an increase in the harvesting effort, thus exhibiting the hydra effect recently reviewed by Abrams (2009). In this way, we generalize the results in previous papers (Seno 2008; Abrams 2009; Liz 2010a). We identify the range of the survivorship and harvesting parameters for which this paradoxical effect occurs when the positive equilibrium is stable, and we provide some numerical results when the equilibrium is unstable. Overall, we conclude that the hydra effect is quite frequent in the population model considered when the survivorship rate is not too high. Moreover, the hydra effect occurs for all positive initial conditions, so it is a highly observable phenomenon; we prove this fact when the equilibrium is stable, and extensive numerical simulations indicate that it is also true in the unstable case.

On the other hand, our results confirm that harvesting can magnify fluctuations in population abundance for relatively high values of the per-capita recruitment. Since our model assumes adult-only harvesting, these results are in agreement with the age truncation effect, which has been documented in several populations (see Anderson et al. (2008), and its references). This is a clear difference with models for single-species populations without adult survivorship, where harvesting typically helps to simplify the dynamics (Goh 1977; May et al. 1978). For stage-structured models, transitions in the complexity of the dynamics due to an increase in adult mortality was observed in laboratory cultures of the flour beetle *Tribolium*, as reported by Dennis et al. (1997).

In accordance with the conclusions stated by Zipkin et al. (2009) for a stage-structured discrete population model with two age classes (juveniles and adults), harvesting leads to instability in our model when both maximum per capita recruitment and adult survivorship are high; moreover, we determine analytically the range of these two parameters for which harvesting can destroy the stability of the positive equilibrium, producing bubbles in the bifurcation diagram (see Theorem 2). But, in addition to this, we observe that variability in the population size can be dramatically enhanced, as the harvesting rate is increased, also for low survivorship rates. Actually, in this case, a population which exhibits a stable period-two regime without harvesting can be driven to a chaotic regime as harvesting increases. Existence of chaos is suggested by numerically computed bifurcation diagrams, in the form of paired period-doubling cascades (Sander and Yorke 2011). This means that the usual route to chaos is reversed in such a way that further increasing harvesting leads the population to a more stable regime again. For some values of the parameters, we are able to prove analytically existence of chaos, which is robust under small perturbations.

We emphasize that the two counterintuitive effects of increasing harvesting studied for equation (2) (bubbling and hydra effect) often co-occur, and the hydra effect can also happen within a chaotic regime. While regarding the phenomenon of bubbling it does not matter whether harvesting occurs prior or after reproduction, the hydra effect is typical from models when mortality precedes density dependence, as already noticed by Abrams (2009) and Seno (2008).

Another by-product of our numerical results is that, while in the Ricker model (without adult survivorship) the positive equilibrium is equal to the mean population size even in the unstable cases, if the species invest some energy in survivorship rather than reproduction then the mean population size is usually greater than the equilibrium.

An interesting open problem is to study how the results in this paper may change when evolution is taken into account. For example, Gyllenberg, Hanski, and Lindström (1996) showed that adaptive adjustment of reproduction in a single-species modeled by a Ricker map may decrease the mean amplitude of oscillations when the positive equilibrium is unstable.

Appendices

A Proof of Theorems 1 and 2

Proof of Theorem 1. As usual, we denote by $h_\gamma(x) = F_\alpha((1-\gamma)x)$, in such a way that equation (2) can be written as

$$x_{n+1} = h_\gamma(x_n).$$

Statement (i) is a consequence of the fact that $\gamma \geq \gamma^*$ implies that $h_\gamma(x) < x$ for all $x > 0$. Thus, all solutions of (2) starting at a positive initial condition are decreasing and converge to zero.

If $\gamma < \gamma^*$ then $h'_\gamma(0) = (1-\gamma)F'_\alpha(0) > 1$, so that zero is unstable. Formula (6) is easy to obtain from the equality $h_\gamma(x) = x$. Thus, statement (ii) is proved.

Assertion (iii) is derived from Corollary 2.9 in (El-Morshedy and Jiménez-López 2008), using Proposition 1 (b), analogously to the proof of Theorem 1 in (Liz and Franco 2010).

Finally, statement (iv) is a direct consequence of the criterion for linear stability. □

Proof of Theorem 2. By Theorem 1, we know that, for a fixed $r > r_0(\gamma)$, the positive equilibrium K_γ of (2) changes its asymptotic stability when

$$r = \ln\left(\frac{1-(1-\gamma)\alpha}{(1-\alpha)(1-\gamma)}\right) + \frac{2}{1-\alpha(1-\gamma)}. \tag{13}$$

Let us consider the function

$$G(\alpha,\gamma) = \frac{2}{1-\alpha(1-\gamma)} + \ln\left(\frac{1-(1-\gamma)\alpha}{(1-\alpha)(1-\gamma)}\right) - r. \tag{14}$$

An application of the Implicit Function Theorem allows us to ensure that equation (13) defines α as a smooth function of γ and

$$\alpha'(\gamma) = -\frac{\partial G/\partial\gamma}{\partial G/\partial\alpha}\,. \tag{15}$$

First we prove that, for every fixed $\gamma \in [0,1)$, there is at most one value of $\alpha \in [0,1]$ for which (13) holds. Indeed, let us fix $\gamma \in [0,1)$ We introduce the variable $z = 1-\alpha(1-\gamma)$, $\alpha \in [0,1]$. With this notation, (13) is equivalent to

$$g(z) := \frac{2}{z} + \ln\left(\frac{z}{z-\gamma}\right) = r. \tag{16}$$

Since

$$g'(z) = \frac{-2}{z^2} + \frac{1}{z} - \frac{1}{z-\gamma}\,,$$

and $0 < z - \gamma \leq z$, it follows that g is decreasing on $(0, 1]$. It is hence clear that equation (16) has at most one solution $z(\gamma)$. Therefore, there is at most one solution of (13) given by

$$\alpha(\gamma) = \frac{1 - z(\gamma)}{1 - \gamma}.$$

We notice that, for $\gamma = 0$, this solution exists and it is given by

$$\alpha(0) = 1 - z(0) = 1 - \frac{2}{r}.$$

On the other hand, (15) leads to

$$\alpha'(\gamma) = \frac{(1-\alpha)\,(3\alpha(1-\gamma) - 1)}{(1-\gamma)(2 - \gamma + \alpha(\gamma^2 + \gamma - 2))}\,.$$

The denominator of this fraction is always positive, and hence $\alpha'(\gamma) < 0$ if and only if $3\alpha(1-\gamma) < 1$.

In particular, $\alpha'(0) \leq 0$ implies that $\alpha'(\gamma) < 0$ for all $\gamma \in (0, 1)$. In this case, there is not primary bubbling because α is a one-to-one function of γ. Thus we need $\alpha'(0) > 0$, which is equivalent to $\alpha(0) > 1/3$. In this case, α is an increasing function of γ until it intersects the increasing curve $\gamma = 1 - 1/(3\alpha)$ at a point $\bar{\gamma} \in (0, 1 - e^{2-r})$. Notice that $\alpha(\gamma)$ is always decreasing at $\gamma = 1 - e^{2-r}$, since this corresponds to the case $\alpha = 0$, and then

$$\alpha'(1 - e^{2-r}) = \frac{-1}{(2-\gamma)(1-\gamma)} < 0.$$

Thus, there are two points where the stability of K_γ changes if and only if $\alpha \in (\alpha_1(r), \alpha_2(r))$, where

$$\alpha_1(r) = \alpha(0) = 1 - \frac{2}{r} \quad ; \quad \alpha_2(r) = \alpha(\bar{\gamma}) = \frac{e^{r-3}}{2 + e^{r-3}}\,.$$

To complete the proof, we emphasize that a necessary condition for the existence of primary bubbling is $\alpha_1(r) > 1/3$, which is equivalent to $r > 3$. □

B Chaotic Dynamics and Strictly Turbulent Functions

In this appendix, we give the precise definition of chaos, some direct consequences of this definition, and a mechanism to detect chaotic dynamics. As usual, we denote by $\mathbf{Z}$ and $\mathbf{R}$ the set of integer and real numbers respectively.

Definition 4 Consider (X, d) a metric space and let $\psi : \mathcal{D}_\psi \to X$ be a continuous map with $\mathcal{D} \subset \mathcal{D}_\psi$. We say that ψ induces **chaotic dynamics on two symbols** on the set $\mathcal{D}$ if there exist two disjoint compact sets $\mathcal{K}_0, \mathcal{K}_1 \subset \mathcal{D}$ such that, for each two-sided sequence $\{s_i\}_{i\in\mathbf{Z}} \in \{0,1\}^{\mathbf{Z}}$, there exists a corresponding sequence $\{\omega_i\}_{i\in\mathbf{Z}} \in \mathcal{D}^{\mathbf{Z}}$ such that

$$\omega_i \in \mathcal{K}_{s_i} \quad \text{and} \quad \omega_{i+1} = \psi(\omega_i) \quad \text{for all } i \in \mathbf{Z}, \tag{17}$$

and, whenever $\{s_i\}_{i\in\mathbf{Z}}$ is a k-periodic sequence (that is, $s_{i+k} = s_i$, $\forall\, i \in \mathbf{Z}$) for some $k \geq 1$, there exists a k-periodic sequence $\{\omega_i\}_{i\in\mathbf{Z}} \in \mathcal{D}^{\mathbf{Z}}$ satisfying (17).

In contrast with other definitions of chaos, we can say that if a map is chaotic according Definition 4, then it is also chaotic in the sense of Block-Coppel and also in the sense of "coin-tossing" (Kirchgraber and Stoffer 1989; Aulbach and Kieninger 2001). Moreover, Definition 4 guarantees the existence of an invariant compact set $\Lambda \subset \mathcal{D}$ such that $\psi|_\Lambda$ is semi-conjugate to the Bernoulli shift on two symbols, topologically transitive, and has sensitive dependence on initial conditions, (see Lemma 5.1 in (Pireddu and Zanolin 2007) or Theorem 2.2 in (Medio, Pireddu and Zanolin 2009)).
To prove the presence of chaotic dynamics we will use the notion of strictly turbulent function. More precisely,

Definition 5 Let $f : I \longrightarrow I$ be a continuous function defined on an interval $I \subset \mathbf{R}$. We say that f is strictly turbulent if there exist two disjoint compact intervals J_1, J_2 such that $J_1 \cup J_2 \subset f(J_1)$ and $J_1 \cup J_2 \subset f(J_2)$.

It was proven in Proposition II.3.15 in (Block and Coppel 1992) (see also Theorem 2.3 in (Medio, Pireddu and Zanolin 2009)) that every strictly turbulent function induces chaotic dynamics on two symbols.

Next we apply the previous results to equation (2). Consider equation

$$x_{n+1} = F_\alpha((1-\gamma)x_n) =: G_\alpha(x_n), \tag{18}$$

where $F_\alpha(x) = \alpha x + (1-\alpha)xe^{r(1-x)}$, and define $H_\alpha(x) = G_\alpha^2(x) = G_\alpha(G_\alpha(x))$. Clearly, H_α is strictly turbulent if there exist four constants $0 < a_1 < b_1 < a_2 < b_2$ satisfying that

$$H_\alpha(a_1) < a_1;\ H_\alpha(b_1) > b_2;\ H_\alpha(a_2) > b_2;\ H_\alpha(b_2) < a_1. \tag{19}$$

It follows from straightforward computations that the four inequalities in (19) hold for the parameters $\alpha = 0.02$, $\gamma = 0.55$, $r = 4$ and the constants $a_1 = 1.53$, $b_1 = 2.45$, $a_2 = 2.5$, and $b_2 = 4.25$. Indeed, we have that $H_\alpha(1.53) = 1.47486$, $H_\alpha(2.45) = 4.79068$, $H_\alpha(2.5) = 4.69515$ and $H_\alpha(4.25) = 1.49457$. In this way, we can conclude that under (19), Eq. (18) has infinitely many periodic points and there is a compact invariant set Γ such that $G_\alpha|_\Gamma$ is topologically transitive and has sensitive dependence on initial conditions. In this case, $\Gamma = \Lambda \cup G_\alpha(\Lambda)$, where Λ is the corresponding invariant set for H_α (see the comment below Definition 4). At this point it is also clear the robustness of our method under small perturbations, since it works for all values of (α, γ, r) for which (19) still holds.

Acknowledgements

We are very grateful to the Associate Editor Prof. S. Schreiber and two anonymous reviewers of a first draft of this paper. Their comments and insightful critique helped us very much to improve the paper.

E. Liz was supported in part by the Spanish Ministry of Science and Innovation and FEDER, grant MTM2010–14837. A. Ruiz-Herrera was supported by the Spanish Ministry of Science and Innovation grant MTM2008–02502.

The authors started to work on the paper while the second author was visiting the University of Vigo (Spain). It is his pleasure to thank the Departamento de Matemática Aplicada II for its kind hospitality.

References

Abrams PA (2009) When does greater mortality increase population size? The long story and diverse mechanisms underlying the hydra effect. Ecol Lett 12:462–474.

Ambika G, Sujatha NV (2000) Bubbling and bistability in two parameter discrete systems. Pramana- J Phys 54:751–761.

Anderson CNK *et al.* (2008) Why fishing magnifies fluctuations in fish abundance. Nature 452:835–839.

Aulbach B, Kieninger B (2001) On three definitions of chaos. Nonlinear Dyn Syst Theory 1:23–37.

Bier M, Bountis TC (1984) Remerging Feigenbaum trees in dynamical systems. Phys Lett A 104:239–244.

Block LS, Coppel WA (1992) Dynamics in one dimension. Lecture Notes in Mathematics 1513. Springer-Verlag, Berlin.

Clark CW (1990) [First Edition: 1976] Mathematical bioeconomics: the optimal management of renewable resources (Second Edition). John Wiley & Sons, Hoboken, New Jersey.

Dennis B, Desharnais RA, Cushing JM, Costantino RF (1997) Transitions in population dynamics: equilibria to periodic cycles to aperiodic cycles. J Anim Ecol 66:704–729.

Devaney RL (1989) An introduction to chaotic dynamical systems (Second Edition). Perseus Books, Reading, Massachusetts.

El-Morshedy HA, Jiménez-López V (2008) Global attractors for difference equations dominated by one-dimensional maps. J Difference Equ Appl 14:391–410.

Goh BS (1977) Stability in a stock-recruitment model of an exploited fishery. Math Biosciences 33:359–372.

Gyllenberg M, Hanski I, Lindström T (1996) A predator-prey model with optimal suppression of reproduction in the prey. Math Biosci 134:119–152.

Gyllenberg M, Osipov AV, Söderbacka G (1996) Bifurcation analysis of a metapopulation model with sources and sinks. J. Nonlinear Sci 6:329–366.

Hastings A (1997) Population biology. Concepts and models. Springer-Verlag, New York.

Kirchgraber U, Stoffer D (1989) On the definition of chaos. Z Angew Math Mech 69:175–185.

Liz E (2010a) How to control chaotic behaviour and population size with proportional feedback. Phys Lett A 374:725–728.

Liz E (2010b) Complex dynamics of survival and extinction in simple population models with harvesting. Theor Ecol 3:209–221.
Liz E, Franco D (2010) Global stabilization of fixed points using predictive control. Chaos 20:023124, 9 pp.
May RM (1976) Simple mathematical models with very complicated dynamics. Nature 261:459 - 467.
May RM, Beddington JR, Horwood JW, Shepherd JG (1978) Exploiting natural populations in an uncertain world. Math Biosci 42:219–252.
Medio A, Pireddu M, Zanolin F (2009) Chaotic dynamics for maps in one and two dimensions: a geometrical method and applications to economics. Internat J Bifur Chaos Appl Sci Engrg 19:3283–3309.
Newman TJ, Antonovics J, Wilbur HM (2002) Population dynamics with a refuge: fractal basins and the suppression of chaos. Theor Popul Biol 62:121–128.
Pireddu M, Zanolin F (2007) Cutting surfaces and applications to periodic points and chaotic-like dynamics. Topol Methods Nonlinear Anal 30:279–319. Correction (2009) in Topol Methods Nonlinear Anal 33:395.
Ricker WE (1954) Stock and recruitment. J Fish Res Bd Can 11:559–623.
Sander E, Yorke JA (2011) Period-doubling cascades galore. Ergodic Theory Dynam Systems 31:1249–1267.
Schreiber SJ (2001) Chaos and population disappearances in simple ecological models. J Math Biol 42:239–260.
Schreiber SJ (2003) Allee effect, extinctions, and chaotic transients in simple population models. Theor Popul Biol 64:201–209.
Schreiber SJ (2007) Periodicity, persistence, and collapse in host-parasitoid systems with egg limitation. J Biol Dyn 1:273–288.
Seno H (2008) A paradox in discrete single species population dynamics with harvesting/thinning. Math Biosci 214:63–69.
Sieber M, Hilker F (In press) The hydra effect in predator-prey models. J Math Biol, available online, DOI: 10.1007/s00285-011-0416-6.
Sinha S, Parthasarathy S (1996) Unusual dynamics of extinction in a simple ecological model. Proc Natl Acad Sci USA 93:1504–1508.
Stone L (1993) Period-doubling reversals and chaos in simple ecological models. Nature 365:617–620.
Stone L, Hart D (1999) Effects of immigration on the dynamics of simple population models. Theor Popul Biol 55:227–234.
Thamilmaran K, Lakshmanan M (2002) Classification of bifurcations and routes to chaos in a variant of Murali-Lakshmanan-Chua circuit. Internat J Bifur Chaos Appl Sci Engrg 12:783–813.
Thieme HR (2003) Mathematics in Population Biology. Princeton University Press.
Thunberg H (2001) Periodicity versus chaos in one-dimensional dynamics. SIAM Rev 43:3–30.
Vandermeer J (1997) Period 'bubbling' in simple ecological models: Pattern and chaos formation in a quartic model. Ecological Modelling 95:311 317.
Yakubu A-A, Li N, Conrad JM, Zeeman M-L (2011) Constant proportion

harvest policies: Dynamic implications in the Pacific halibut and Atlantic cod fisheries. Math Biosci 232:66–77
Zipkin EF, Kraft CE, Cooch EG, Sullivan PJ (2009) When can efforts to control nuisance and invasive species backfire? Ecological Applications 19:1585–1595.